Lewis Acidity in Transition-Metal-Doped Microporous Aluminophosphates**

Furio Corà,* Iman Saadoune, and C. Richard A. Catlow

The origin of Lewis acidity in microporous framework oxides, such as zeolites and aluminophosphates (AlPOs) has been extensively debated.[1,2] Experimental temperature-programmed desorption (TPD) and calorimetric data probing the interaction of Lewis basic molecules, such as ammonia or acetonitrile, with doped AlPOs, show the presence of two distinct adsorption sites, attributed in one case to the Brønsted and in the other to the Lewis acid sites within the framework.[3,4] When transition metal ions are incorporated into the framework of AlPOs during synthesis, the Lewis acidity is likely to be associated with the transition metal centers. Not all the dopant ions, however, interact in the same way with Lewis bases in metal–AlPO compounds; for instance, AlPOs containing Ni^{2+} ions have been shown to possess much less pronounced Lewis acidity than their Co and Mn analogues.[3] The cause of the different behavior is still unclear. Given the interest in doped AlPOs for their applications in heterogeneous catalysis,[5,6] the desire to understand the mechanism by which the Lewis acidity operates and influences the interaction of reactants with the active sites within the framework is a topic of primary importance.

In this communication we investigate, with periodic ab initio quantum mechanical (QM) calculations, the electronic distribution of a set of $2+$ and $3+$ transition metal ions, isomorphously substituted for Al in the framework of AlPO-34. We use the results of our calculations to examine the possible origin of the Lewis acidity in the doped aluminophosphates. The factors controlling the Lewis acidity will be discussed by examining the calculated electronic distribution of the transition metal dopants; in particular, we shall consider the orientation of the empty d atomic orbitals (AOs) on the metal site.

The doped AlPO-34 framework employed in these calculations is a supercell model in which one dopant ion is included in each unit cell of the host framework (composed of 36 atoms, or $6\,AlPO_4$ formula units). Even at this high concentration, compared to the level of doping achievable experimentally, the dopant ions are separated approximately 10 Å from each other, and thus represent non-interacting defect centers. The supercell model describes correctly the extended nature of the solid catalyst; the crystal field and the structural strain caused by the crystalline matrix on the substitutional ion are therefore included in the computational model.

[*] Dr. F. Corà, I. Saadoune, Prof. C. R. A. Catlow
Davy Faraday Research Laboratory
The Royal Institution of Great Britain
21 Albemarle Street, London W1S 4BS (UK)
Fax: (+44) 20-7629-3569
E-mail: furio@ri.ac.uk

[**] We would like to thank the EPSRC for funding this research project; F.C. acknowledges a grant from the Royal Society for the purchase of computer equipment.

The dopant ions investigated are Cr^{2+}, Mn^{2+}, Fe^{2+}, Co^{2+}, Ni^{2+}; Cr^{3+}, Mn^{3+}, Fe^{3+}, and Co^{3+}, each replacing one Al^{3+} ion of the host framework. The low-valent $(2+)$ ions are charge-compensated by protonating one of the framework oxygen ions that is a nearest neighbor to the dopant, as shown in Figure 1.

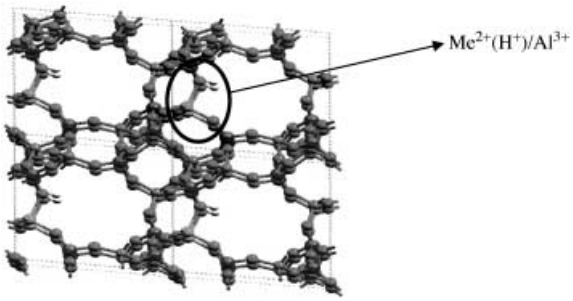

Figure 1. Structure of a $2+$ dopant ion, charge-compensated by an acid proton, that replaces a framework Al^{3+} ion in ALPO-34, described using periodic boundary conditions.

Since the dopants examined are open-shell transition metal ions, we performed our calculations at the Unrestricted Hartree–Fock (UHF) level; this Hamiltonian employs the exact expression of exchange forces, which are important for a correct representation of the unpaired electrons. Calculations for the Ni^{2+} dopant have also been repeated with a B3LYP density functional Hamiltonian, employing the hybrid exchange functional proposed by Becke.[7] This functional has been shown both in molecular[7] and in solid-state calculations[8] to provide a very accurate description of the electronic density and energetics of the systems investigated. The calculations have been performed with the latest version of the CRYSTAL code,[9] which includes the analytical evaluation of forces.[10,11] The transition metal ions are described with an 8-64111d41G basis set, available from the online database of the CRYSTAL code.[12] For each dopant ion investigated, we have determined the equilibrium structure by performing a geometry optimization of all the internal coordinates within the unit cell using P1 symmetry. The Lewis acidity properties are calculated for the equilibrium structure of each ion.

In transition-metal-doped AlPOs, the unpopulated and/or partially filled d AOs of the transition metal site are obvious candidates to explain the presence or absence of Lewis acidity in the framework. To investigate this feature we have calculated the total and spin electronic density of each metal dopant in its equilibrium structure; the result is plotted in Figure 2 for the isovalent $3+$ ions, and in Figure 3 for the low-valent $2+$ ions. The plane of the figures is chosen to contain the transition metal dopant, one of its nearest-neighbor oxygen ions (for the $2+$ ions we chose the oxygen ion bonded to the charge-compensating proton), and the next-nearest phosphorus ion bonded to the oxygen ion previously described. In each plot, the continuous and dashed black and green lines are the isodensity levels calculated from the spin density.

Not all of the interstitial space within the microporous framework is accessible to adsorbed molecules: the Pauli

  0044-8249/02/4124-4677 $ 20.00+.50/0

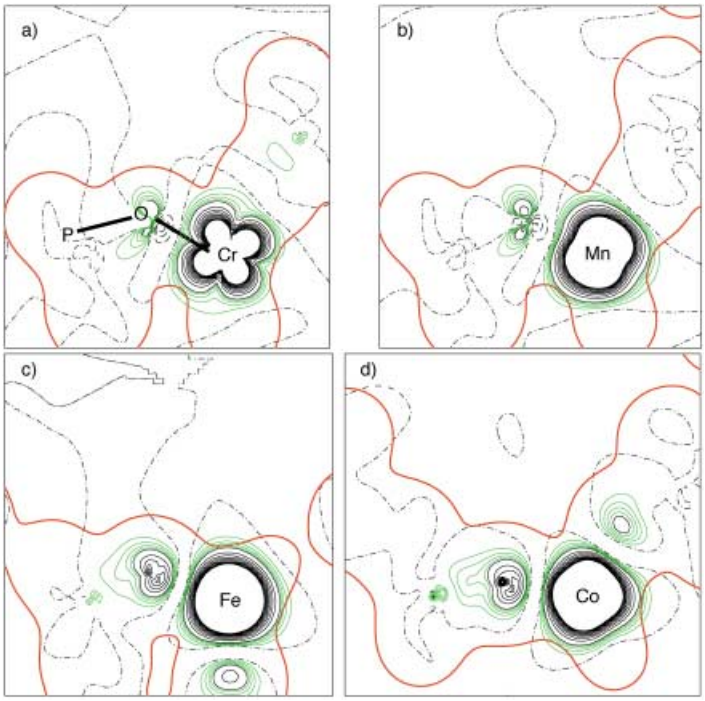

Figure 2. Electron and spin density maps for the isovalent 3+ transition metal ions in AlPO-34. The black and green lines represent the spin density, plotted between −0.05 and +0.05 a.u. at linear steps of 0.005 a.u. (black), and between 0.001 and 0.005 a.u. at linear steps of 0.001 a.u. (green). Continuous and dashed lines refer to positive and negative spin density, respectively. The continuous red line is the isodensity level of 0.01 a.u. calculated from the total electronic density, and represents the effective size of the framework. The substitutional ions are Cr^{3+} (a), Mn^{3+} (b), Fe^{3+} (c), and Co^{3+} (d).

repulsion caused by the overlap between the electronic density of the molecule and of the framework atoms makes the adsorption process energetically unfavorable when the molecule is too close to the framework atoms. How close the adsorbed molecules can approach the framework and its active sites depends therefore on the radial extent of the electronic density of the framework itself. To have an indication of this feature, we have calculated the total electronic density of the doped materials; in Figure 2 and Figure 3 we plot in red the isodensity level of 0.01 a.u., which represents an "effective" framework size beyond which the adsorbed molecules cannot approach the framework ions.

The transition metal ions investigated have a partially filled d shell, with electronic configurations ranging between the d^3 of Cr^{3+} to the d^8 of Ni^{2+}. When they are isomorphously substituted for Al in the AlPO-34 framework, our calculations show that all the transition metal ions investigated are stable in the spin state with highest multiplicity compatible with their count of d electrons. A high-spin state would indeed be expected, because of the low crystal-field splitting caused by the tetrahedral coordination of the transition metal ions; the partially covalent character of the oxygen ligands with the phosphorus ions[13,14] decreases their net charge, and makes the crystal field they create insufficient to stabilize low-spin states on the transition metals.

The spin density of Figure 2 and Figure 3 represents the distribution of the half filled d AOs of the metal dopant. When considering the Lewis acidity of open-shell transition metal ions in the high-spin state, we have to distinguish between ions with less than half filled d AOs (that is, with electronic configuration d^3–d^4), and ions with d AOs that are at least half filled (with electronic configuration d^5–d^8). In the former case the spin density represents the orbitals which are least active towards Lewis acidity: they are half filled, while the other d orbitals are empty and therefore stronger Lewis acids, whereas in the latter case, the spin density represents the d orbitals responsible for the Lewis acidity: they are half filled, while the remaining levels are all occupied by two electrons, and hence inactive for Lewis acidity.

We clearly see in Figure 2 and Figure 3 that the orientation and radial extent of the spin density differs according to the electronic configuration of the dopant ion. As a result, the extent of spin density that spills outside the Pauli repulsion area (red line) varies considerably among the dopants. In particular, we notice that the Lewis-active orbitals of the Ni^{2+} ion are oriented along the framework; a molecule inside the microporous cages of a Ni-doped AlPO will therefore be subject to Pauli repulsion from the framework before having

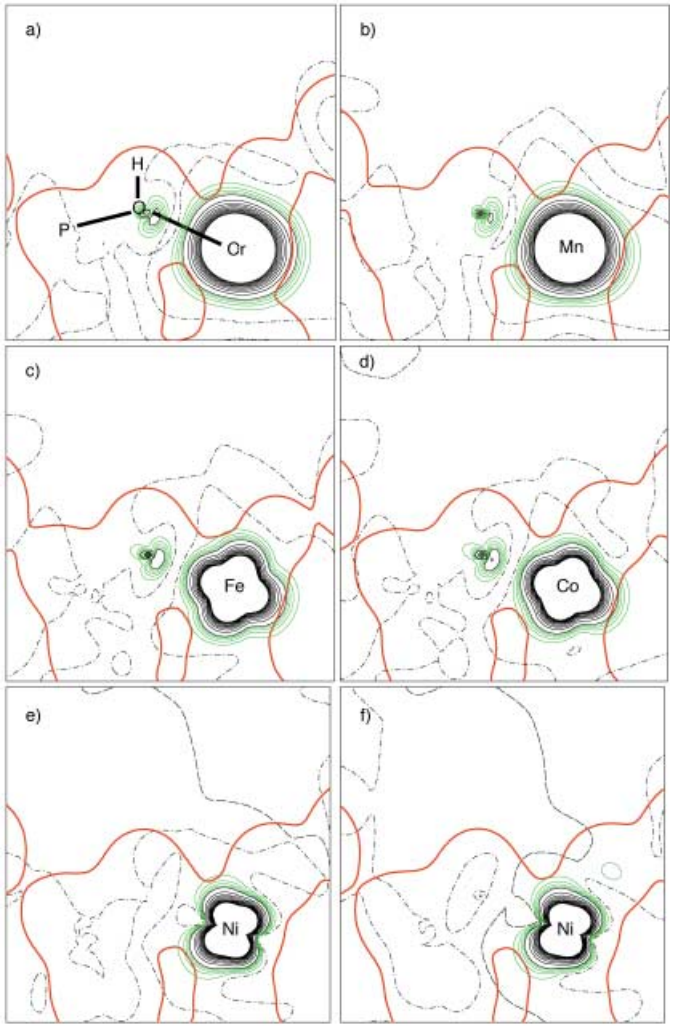

Figure 3. Electron and spin density maps for the low-valent 2+ transition metal ions in AlPO-34. Symbols and units as in Figure 2. The substitutional ions are Cr^{2+} (a), Mn^{2+} (b), Fe^{2+} (c), Co^{2+} (d), and Ni^{2+} (e). The plot (f) refers to the solution for Ni^{2+}, calculated with the B3LYP Hamiltonian.

  0044-8249/02/4124-4678 $ 20.00+.50/0

an effective interaction with the Lewis-active orbitals of the Ni ion. This is not the case, however, for Mn, Fe, and Co dopant ions; molecules in Mn, Fe, and Co-doped materials can undergo an appreciable chemical interaction with the Lewis-active orbitals before being repelled by the framework. We consider that this result explains effectively the origin of the Lewis acidity in the latter frameworks, and its absence in the Ni-doped materials, in agreement with the experimental results of reference[3]. The presence of empty d states on the transition metal site, oriented in a perpendicular direction to the framework structure, is necessary to initiate a Lewis acid–base interaction with adsorbed molecules.

To investigate whether this result depends on the Hamiltonian employed in the calculations, we have repeated the study of Ni-AlPO-34 with the B3LYP density functional. We find no significant qualitative changes, suggesting that our results have general validity.

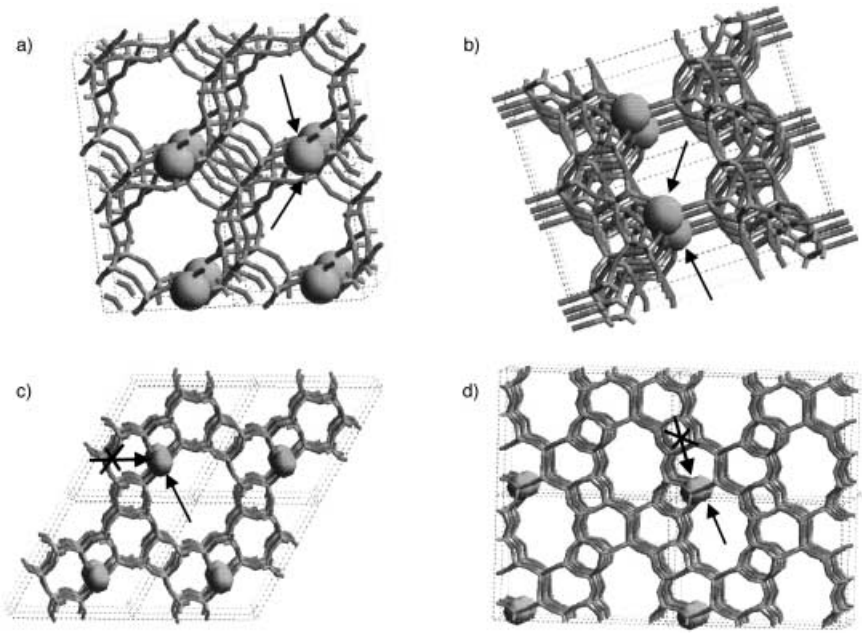

Figure 4. Structural environment of the cationic framework sites in different zeotypic framework topologies: a) chabasite (AlPO-34), b) ferrierite, c) AlPO-5, and d) AlPO-11. The two-dimensional open space in chabasite and ferrierite is visible, which allows "attack from behind" of the framework ions, along with the one-dimensional character of AlPO-5 and AlPO-11, which prevents such a form of attack.

It is also important to notice in Figure 3 that for the 2+ dopant ions, the spilling of the spin density outside the Pauli repulsion area is most effective on the side of the framework opposite to the proton. This feature suggests that the interaction of Lewis bases with the 2+ transition metal ions is most effective when the molecule can approach the framework from the side opposite to the protonated oxygen ion, while interaction of the adsorbed molecule with the Brønsted acid proton prevents a Lewis-type acid–base interaction with the transition metal ion. We refer to this structural requirement as an "attack from behind" of the Lewis-basic molecule to the transition metal dopant. This suggestion of our computational work is indirectly supported by experimental work on Co^{2+}-doped AlPOs,[15,16] in which the authors found that to achieve complexation (Lewis interaction) of the framework Co^{2+} ions by acetonitrile, the Co–OH bond between the Co^{2+} ion and the Brønsted acid OH group must be broken, that is, that Lewis and Brønsted acid interactions are mutually exclusive. Such a structural property of Lewis-type interactions is able to differentiate the Lewis acidity of different AlPO frameworks. We expect, in fact, that the transition metal ions will be more Lewis active when they are located in open regions of a framework, where the space behind the dopant and the protonated oxygen ion is not protected by other ions of the framework. Instead, the structures are expected to be less Lewis-active when the dopant and the protonated oxygen ion cannot be approached from behind by adsorbed molecules, as is the case when the transition metal dopant is located in a double-walled structural unit. As a general rule, we predict therefore that the microporous polymorphs of zeolites and AlPOs with intersecting channels, or with single walls between large cages, such as the Chabasite (AlPO-34 and its closely related AlPO-18) and Ferrierite framework topologies (Figure 4a,b), will have more active Lewis acid sites than those framework structures with one-dimensional channels made of "double-wall" building units, such as those found in the AlPO-5 and AlPO-11 structures (Figure 4c,d). This result may explain why, experimentally, the Lewis-acidic behaviour of Co-AlPO-5 towards the adsorption of acetonitrile was found to be similar to that of Co-AlPO-11,[17] but different from that of Co-AlPO-18.[15,16] We leave open for further experimental verifications this prediction of the computational work.

In conclusion, results of our QM calculations on transition-metal-doped AlPO-34 suggest an electronic explanation for the Lewis acidity of these materials. This feature requires the presence of empty d states on the transition metal site, oriented in a perpendicular direction to the framework structure, which is necessary to initiate a Lewis acid–base interaction with adsorbed molecules. Attack "from behind" of Lewis basic molecules to 2+ dopant ions is favored, and is expected to yield stronger Lewis acidity for polymorphs with single-wall framework structure, rather than polymorphs with one-dimensional channels and composed only of double-walled structural units.

Received: August 13, 2002
Revised: September 30, 2002 [Z19959]

[1] H. G. Karge, V. Dondur, *J. Phys. Chem.* **1990**, *94*, 765.
[2] H. G. Karge, V. Dondur, J. Weitkamp, *J. Phys. Chem.* **1991**, *95*, 283.
[3] G. Lischke, B. Parlitz, U. Lohse, E. Schreier, R. Fricke, *Appl. Catal. A* **1998**, *166*, 351.
[4] "Zeolites and Related Microporous Materials: State of the Art 1994": J. Jänchen, M. J. Haanepen, M. P. J. Peeters, J. H. M. C. van Wolput, J. P. Wolthuizen, J. H. C. van Hooff, *Stud. Surf. Sci. Catal.* **1994**, 84.
[5] A. Corma, H. García, *Catal. Today* **1997**, *38*, 257.

  0044-8249/02/4124-4679 $ 20.00+.50/0

[6] J. M. Thomas, *Angew. Chem.* **1999**, *111*, 3800; *Angew. Chem. Int. Ed.* **1999**, *38*, 3588.
[7] A. D. Becke, *J. Chem. Phys.* **1993**, *98*, 5648.
[8] J. Muscat, A. Wander, N. M. Harrison, *Chem. Phys. Lett.* **2001**, *342*, 397.
[9] V. R. Saunders, R. Dovesi, C. Roetti, M. Causà, N. M. Harrison, R. Orlando, C. M. Zicovich-Wilson, K. Doll, B. Civalleri, CRYSTAL User's Manual, Univ. of Torino, Torino, **1998** and **2001**.
[10] K. Doll, V. R. Saunders, N. M. Harrison, *Int. J. Quantum Chem.* **2001**, *82*, 1.
[11] B. Civalleri, Ph. D'Arco, R. Orlando, V. R. Saunders, R. Dovesi, *Chem. Phys. Lett.* **2001**, *348*, 131.
[12] http://www.chimifm.unito.it/teorica/crystal/Basis_Sets/mendel.html.
[13] F. Corà, C. R. A. Catlow, *J. Phys. Chem. B* **2001**, *105*, 10278.
[14] F. Corà, C. R. A. Catlow, A. D'Ercole, *J. Mol. Catal. A* **2001**, *166*, 87.
[15] J. Chen, J. M. Thomas, G. Sankar, *J. Chem. Soc. Faraday Trans.* **1994**, *90*, 3455.
[16] P. A. Barrett, G. Sankar, R. H. Jones, C. R. A. Catlow, J. M. Thomas, *J. Phys. Chem. B* **1997**, *101*, 9555.
[17] J. Jänchen, M. P. J. Peeters, J. H. M. C. van Wolput, J. P. Wolthulzen, J. H. C. van Hooff, *J. Chem. Soc. Faraday Trans.* **1994**, *90*, 1033.

Total Synthesis of (±)-Wortmannin**

Takashi Mizutani, Shinobu Honzawa, Shin-ya Tosaki, and Masakatsu Shibasaki*

Wortmannin (**1**) is a potent and specific phosphoinositide 3-kinase (PI3K) inhibitor with a low nanomolar IC_{50} value[1] that was originally isolated from *Penicillium Wortmannii* as an anti-inflammatory and antibiotic agent.[2] Wortmannin (**1**) acts by covalently binding Lys802 in the ATP binding pocket of PI3K through nucleophilic attack of the Lys amino group at the C21 position of **1**.[3] PI3K is an important enzyme that functions in signal transduction pathways, and is a potential target for preventing proliferation of cancer cells.[4] Unfortunately, **1** has not yet been applied to medical use because of its high toxicity. Thus, wortmannin derivatives, which possess more potent inhibitory activity against PI3K and have less general toxicity, are necessary for the development of new antitumor drugs. In addition to the medicinal aspect, the challenging structural features of **1**, namely an allylic quaternary carbon center and a furanocyclohexadienone lactone unit, are very attractive from a synthetic point of view. In 1996, we reported the first chemical synthesis of **1** from hydrocortisone.[5] Following this primary achievement, we planned to develop a direct total synthesis of **1**, which would hopefully lead to many more derivatives. Here, we report the first direct total synthesis of (±)-**1** using an intramolecular Heck reaction for stereoselective construction of an allylic quaternary carbon center (Scheme 1)[6] and a diosphenol–Claisen rearrangement (Scheme 3)[7] as key steps.

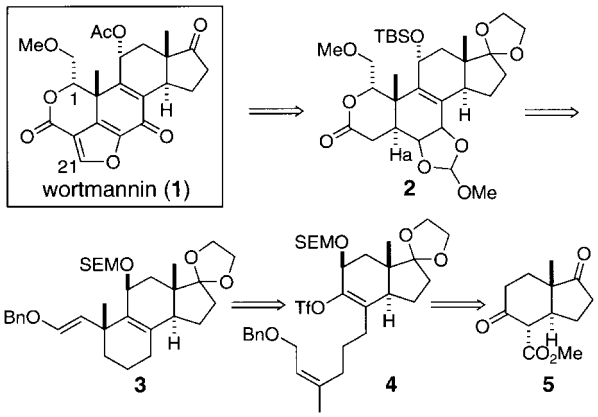

Scheme 1. Retrosynthesis of (±)-wortmannin. SEM = 2-(trimethylsilyl)-ethoxymethyl; TBS = *tert*-butyldimethylsilyl; Tf = trifluoromethanesulfonyl; Bn = benzyl.

Our synthesis began with alkenyl triflate **6**, which was synthesized from compound **5**, and obtained as a racemate[8] in eight steps and in 27% overall yield (Scheme 2).[6c] After conversion of **6** into the SEM-protected ether **7** (87%), it was chemoselectively coupled with **8** by the Suzuki method to give **4** (64%).[9] An intramolecular Heck reaction of **4** afforded

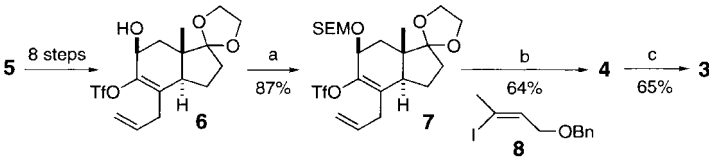

Scheme 2. Synthesis of enol ether **3**. a) SEMCl, 2,6-lutidine, nBu$_4$NI, CH_2Cl_2, 40°C; b) 9-BBN, THF, RT then **8**, [$PdCl_2$(dppf)], K_3PO_4, THF/DMF, 60°C; c) 10 mol% of $Pd(OAc)_2$, 22 mol% of 1,3-bis(diphenylphosphanyl)propane, 1.0 equiv of nBu$_4$NBr, 2.5 mol equiv of K_2CO_3, toluene, 100°C, 17 h. SEMCl = 2-(trimethylsilyl)ethoxymethyl chloride, 9-BBN = 9-borabicyclo[3.3.1]nonane, dppf = 1,1′-bis(diphenylphosphanyl)ferrocene.

enol ether **3** in 65% yield and in excellent diastereoselectivity (β-Me:α-Me = 18:1). It is noteworthy that the stereochemistry of the β-SEM ether in **4** plays a crucial role in the excellent stereoselectivity achieved by the Heck reaction.[6] Unfortunately, the use of the epimer, the α-SEM ether, afforded the undesired (α-Me) isomer as the major product.

Removal of the SEM group, followed by oxidation and reduction, produced α-allylic alcohol **9** (3 steps) together with the β alcohol (Scheme 3). The β-alcohol can be recycled by conventional methods. After protection of **9** as the TBS ether to give **10**, oxidation of the enol ether with 2.5 mol% of OsO_4 and 1.5 equivalents of NMO gave the hydroxyaldehyde, which was then reduced with $LiAlH_4$ to give the desired diol **11**

[*] Prof. Dr. M. Shibasaki
Graduate School of Pharmaceutical Sciences
The University of Tokyo
Hongo, Bunkyo-ku, Tokyo 113-0033 (Japan)
Fax: (+81) 3-5684-5206
E-mail: mshibasa@mol.f.u-tokyo.ac.jp
T. Mizutani, S. Honzawa, S.-y. Tosaki
Graduate School of Pharmaceutical Sciences
The University of Tokyo (Japan)

[**] We thank Dr. Yuzuru Matsuda (Kyowa Hakko Co., Ltd) for kindly supplying a sample of wortmannin. This work was financially supported by CREST, JST, and RFTF. T.M. thanks the Japan Society for the Promotion of Science (JSPS) for a research fellowship.

Supporting information for this article is available on the WWW under http://www.angewandte.org or from the author.

  0044-8249/02/4124-4680 $ 20.00+.50/0